



HAL
open science

Sequential Appearance and Isolation of a SARS-CoV-2 Recombinant between Two Major SARS-CoV-2 Variants in a Chronically Infected Immunocompromised Patient

Emilie Burel, Philippe Colson, Jean-Christophe Lagier, Anthony Levasseur, Marielle Bedotto, Philippe Lavrard-Meyer, Pierre-Edouard Fournier, Bernard La Scola, Didier Raoult

► To cite this version:

Emilie Burel, Philippe Colson, Jean-Christophe Lagier, Anthony Levasseur, Marielle Bedotto, et al.. Sequential Appearance and Isolation of a SARS-CoV-2 Recombinant between Two Major SARS-CoV-2 Variants in a Chronically Infected Immunocompromised Patient. *Viruses*, 2022, 14 (6), pp.1266. 10.3390/v14061266 . hal-03823787

HAL Id: hal-03823787

<https://amu.hal.science/hal-03823787>

Submitted on 6 Jul 2023

HAL is a multi-disciplinary open access archive for the deposit and dissemination of scientific research documents, whether they are published or not. The documents may come from teaching and research institutions in France or abroad, or from public or private research centers.



L'archive ouverte pluridisciplinaire **HAL**, est destinée au dépôt et à la diffusion de documents scientifiques de niveau recherche, publiés ou non, émanant des établissements d'enseignement et de recherche français ou étrangers, des laboratoires publics ou privés.



Distributed under a Creative Commons Attribution 4.0 International License

Article

Sequential Appearance and Isolation of a SARS-CoV-2 Recombinant between Two Major SARS-CoV-2 Variants in a Chronically Infected Immunocompromised Patient

Emilie Burel ^{1,2,†}, Philippe Colson ^{1,2,3,†} , Jean-Christophe Lagier ^{1,2,3}, Anthony Levasseur ^{1,2}, Marielle Bedotto ¹, Philippe Lavrard-Meyer ^{1,2,3}, Pierre-Edouard Fournier ^{1,2,4}, Bernard La Scola ^{1,2,3,*}  and Didier Raoult ^{1,2,*}

- ¹ IHU Méditerranée Infection, 19-21 Boulevard Jean Moulin, 13005 Marseille, France; burel.emilie@hotmail.fr (E.B.); philippe.colson@univ-amu.fr (P.C.); jean-christophe.lagier@univ-amu.fr (J.-C.L.); anthony.levasseur@univ-amu.fr (A.L.); marielle.bedotto@gmail.com (M.B.); philippe.lavrard-meyer@ap-hm.fr (P.L.-M.); pierre-edouard.fournier@univ-amu.fr (P.-E.F.)
- ² Microbes Evolution Phylogeny and Infections (MEPHI), Institut de Recherche Pour le Développement (IRD), Aix-Marseille University, 27 Boulevard Jean Moulin, 13005 Marseille, France
- ³ Assistance Publique-Hôpitaux de Marseille (AP-HM), 264 rue Saint-Pierre, 13005 Marseille, France
- ⁴ Vecteurs-Infections Tropicales et Méditerranéennes (VITROME), Institut de Recherche Pour le Développement (IRD), Aix-Marseille University, 27 Boulevard Jean Moulin, 13005 Marseille, France
- * Correspondence: bernard.la-scola@univ-amu.fr (B.L.S.); didier.raoult@univ-amu.fr (D.R.); Tel.: +33-413-732-401 (B.L.S. & D.R.)
- † These authors contributed equally to this work.



Citation: Burel, E.; Colson, P.; Lagier, J.-C.; Levasseur, A.; Bedotto, M.; Lavrard-Meyer, P.; Fournier, P.-E.; La Scola, B.; Raoult, D. Sequential Appearance and Isolation of a SARS-CoV-2 Recombinant between Two Major SARS-CoV-2 Variants in a Chronically Infected Immunocompromised Patient. *Viruses* **2022**, *14*, 1266. <https://doi.org/10.3390/v14061266>

Academic Editors: Judd F. Hultquist, Ramón Lorenzo-Redondo and Egon Anderson Ozer

Received: 21 March 2022

Accepted: 8 June 2022

Published: 10 June 2022

Publisher's Note: MDPI stays neutral with regard to jurisdictional claims in published maps and institutional affiliations.



Copyright: © 2022 by the authors. Licensee MDPI, Basel, Switzerland. This article is an open access article distributed under the terms and conditions of the Creative Commons Attribution (CC BY) license (<https://creativecommons.org/licenses/by/4.0/>).

Abstract: Genetic recombination is a major evolutionary mechanism among RNA viruses, and it is common in coronaviruses, including those infecting humans. A few SARS-CoV-2 recombinants have been reported to date whose genome harbored combinations of mutations from different mutants or variants, but only a single patient's sample was analyzed, and the virus was not isolated. Here, we report the gradual emergence of a hybrid genome of B.1.160 and Alpha variants in a lymphoma patient chronically infected for 14 months, and we isolated the recombinant virus. The hybrid genome was obtained by next-generation sequencing, and the recombination sites were confirmed by PCR. This consisted of a parental B.1.160 backbone interspersed with two fragments, including the spike gene, from an Alpha variant. An analysis of seven sequential samples from the patient decoded the recombination steps, including the initial infection with a B.1.160 variant, then a concurrent infection with this variant and an Alpha variant, the generation of hybrid genomes, and eventually the emergence of a predominant recombinant virus isolated at the end of the patient's follow-up. This case exemplifies the recombination process of SARS-CoV-2 in real life, and it calls for intensifying the genomic surveillance in patients coinfecting with different SARS-CoV-2 variants, and more generally with several RNA viruses, as this may lead to the appearance of new viruses.

Keywords: SARS-CoV-2; variant; recombination; chronic infection; immunosuppression

1. Introduction

A major evolutionary mechanism of RNA viruses is genetic recombination [1,2]. Recombinations are extremely common in coronaviruses and have been implicated in the emergence of several genotypes, including endemic human coronaviruses [3–6]. The involvement of genetic recombination in the origin of SARS-CoV-2 is also suspected [7]. Regarding SARS-CoV-2, coinfection in the same patient with distinct variants has been reported [8–14]. In addition, several studies have described or suspected genetic recombinations for this virus [10,13–25]. However, most of these recombinants have relied solely on the coexistence of signature mutations of different SARS-CoV-2 variants in genomes obtained from a single patient's sample, and they were not isolated in culture. Since

January 2020, our laboratory has screened more than one million respiratory specimens for SARS-CoV-2 infection by real-time reverse transcription-PCR (qPCR) without interruption or limited capacity, including for all patients sampled in our institute and in the Marseille public hospitals [26,27]. This has provided us with sequential samples from multiple patients, and enabled us to detect reinfections, and prolonged or even chronic infections in severely immunocompromised patients [28–30]. Here, we report the gradual emergence of a recombinant SARS-CoV-2 involving two variants in a lymphoma patient chronically infected over a period of 14 months, and the isolation of the recombinant virus in culture.

2. Results

2.1. Chronic SARS-CoV-2-Infection in a Severely Immunocompromised Patient

A 56-year-old immunocompromised male had an uncontrolled SARS-CoV-2 infection for 14 months until death (Supplementary Material: Supplementary Methods and Results). He was diagnosed in 2017 with mixed Hodgkin and follicular lymphoma and was in complete remission of the Hodgkin lymphoma following chemotherapy, and on maintenance therapy. Follicular lymphoma progression led to the administration of lenalidomide plus rituximab in 2021, and pembrolizumab was also administered. Progressive multifocal leukoencephalitis was diagnosed in May 2021. In August 2020, the patient developed severe SARS-CoV-2-associated pneumonia, leading to admission in the intensive care unit. He improved clinically but viral clearance did not occur, and SARS-CoV-2 RNA remained detectable by qPCR on most nasopharyngeal samples collected between September 2020 and December 2021. qPCR was negative in February 2021 but positive when re-tested in April 2021, and then only transiently negative for ≤ 3 days. COVID-19 patient convalescent plasma was administered during hospitalization outside our institute in October 2020 and April 2021, and hydroxychloroquine was administered in July 2021. The history of SARS-CoV-2 infection did not lead to vaccine administration. The patient died unfortunately in December 2021 from the complications of his hematological and neurological diseases.

2.2. Evidence of Hybrids of Variants

After 14 months of infection, we identified a virus whose genome was a hybrid of two known variants, B.1.160 (according to PANGOLIN (Phylogenetic Assignment of Named Global Outbreak Lineages) lineage (<https://cov-lineages.org/resources/pangolin.html>; accessed on 20 October 2021) [31]) (a.k.a. Nextstrain clade (<https://nextstrain.org/>; accessed on 20 October 2021) [32] 20A.EU2, or Marseille-4 [27]) and Alpha (according to the WHO denomination (<https://www.who.int/fr/activities/tracking-SARS-CoV-2-variants>; accessed on 20 October 2021) (a.k.a. 20I or B.1.1.7)) (Figures 1 and 2).

This hybrid genome was obtained from the respiratory samples by next-generation sequencing, as previously described [27]. In addition, the hybrid virus was isolated in culture, as previously described [33]. The hybrid genome sequence consisted of a B.1.160 variant matrix, of which two regions, the first one being located at the 5' tip of the genome and containing the synonymous mutation C913U, and the second one spanning from positions 17,109–18,877 to positions 25,710–27,972, were replaced by those of an Alpha variant (Figures 1 and 2; Supplementary Material: Figures S1 and S2). All eight signature mutations of the Alpha variant were detected in the spike gene in the absence of the S477N mutation that is a signature of the B.1.160 variant. Nucleotide diversity at the 35 positions harboring signature mutations of the Alpha or B.1.160 variants was low (mean (\pm standard deviation) value of $3.1 \pm 6.8\%$) (Figure 2; Supplementary Material: Figures S1 and S2), indicating that the hybrid content of the genome was not explained by a co-infection from the two variants or by contamination. These findings indicated that this mosaic genome was the result of recombinations between parental genomes of the B.1.160 and Alpha variants.

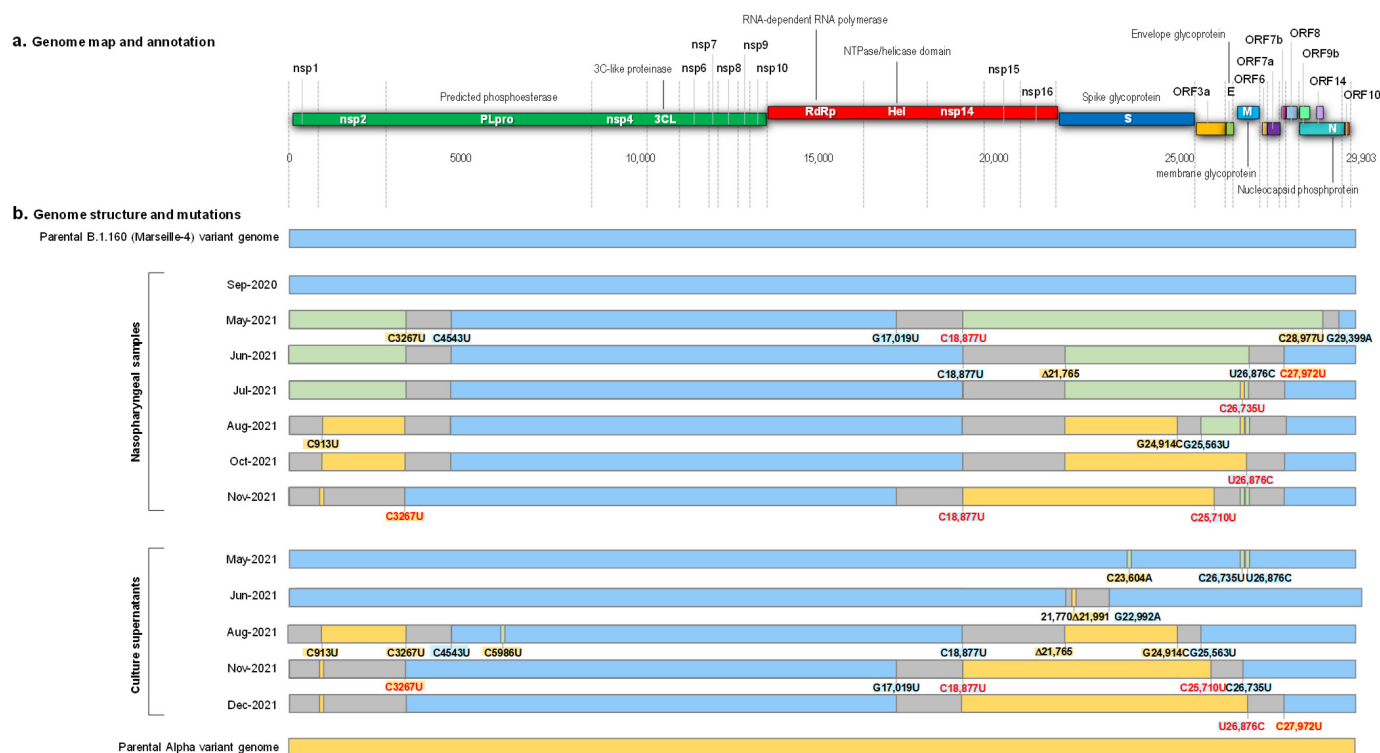


Figure 1. Schematic representation of the structure of the SARS-CoV-2 genomes obtained from the nasopharyngeal samples and from the culture supernatants, as well as of the recombination events over time, in reference to parental genomes of the B.1.160 and Alpha variants. (a) Genome map and annotation; (b) Genome structure and mutations. Blue color of rectangles indicates sequences from a B.1.160 variant; yellow color indicates sequences from an Alpha variant; green color indicates co-detection of sequences from a B.1.160 variant and from an Alpha variant; grey color indicates sequences from indeterminate origin. Signature mutations from the B.1.160 and Alpha variants are indicated by a blue background and a yellow background, respectively. Signature mutations that are absent are indicated by a red font. $\Delta 21,765$: -6 nucleotides; $\Delta 21,991$: -3 nucleotides. Nsp, nonstructural protein; ORF, open reading frame.

By analyzing the sequential samples available from this patient, we were able to determine that he was first infected with the B.1.160 variant, which was epidemic at the time of diagnosis of his infection in September 2020. This variant predominated in our region from August 2020 until January 2021 and was replaced by the Alpha variant, which emerged in December 2020 [27]. SARS-CoV-2 could not be isolated retrospectively from this sample, but its genome was typical of a B.1.160 variant and displayed no significant nucleotide diversity (mean, $0.2 \pm 0.5\%$). It was classified by phylogeny as a B.1.160 variant (Figure 3).

Unfortunately, although SARS-CoV-2 qPCR was still positive in another laboratory in January 2021, the sample was unavailable. Therefore, we were not able to confirm whether Marseille-4 and Alpha variants were co-infecting the patient at this time nor the duration of co-infection, and we did not obtain the genome nor an isolate of the Alpha variant. The closest sample in time to the initial one dated from May 2021, 8 months after the first SARS-CoV-2 diagnosis, and it already demonstrated a mosaicism between genomes of the B.1.160 and Alpha variants (Figures 1 and 2).

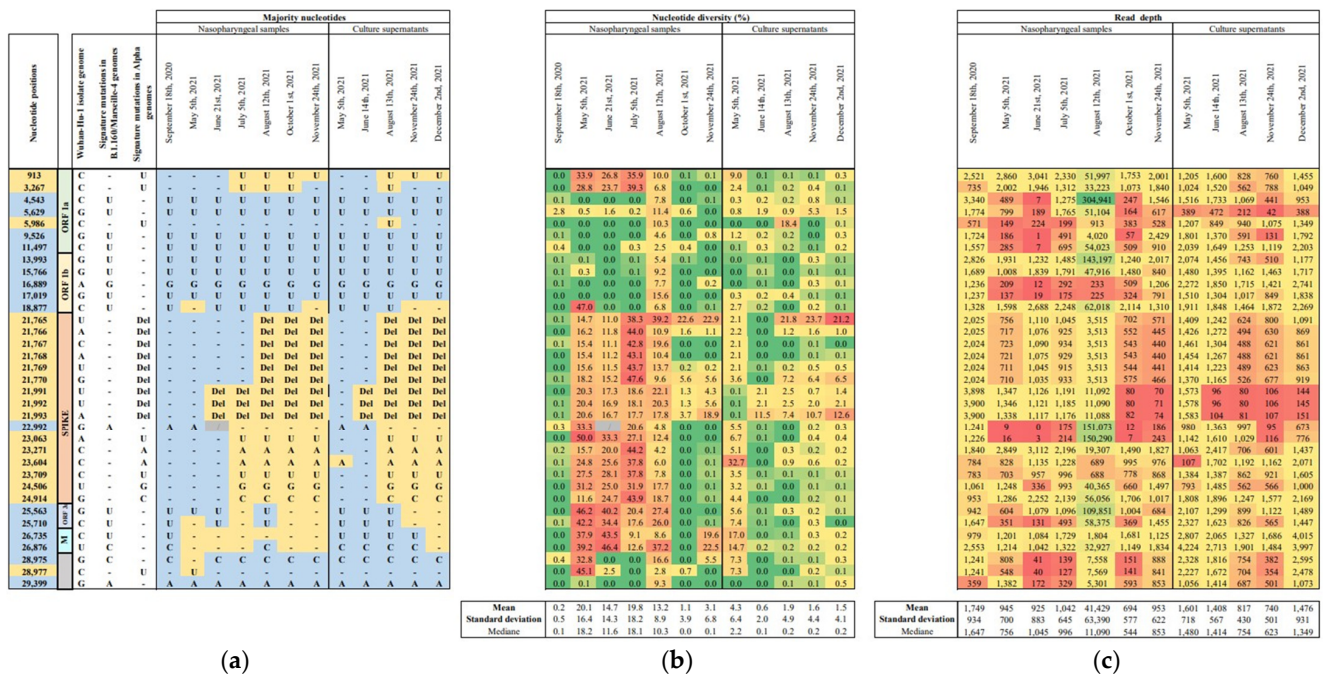


Figure 2. Majority nucleotide diversity (a) and sequencing depth (c) for sequences obtained from the respiratory samples and the culture supernatant at nucleotide positions of the SARS-CoV-2 genome that harbor signature mutations of the B.1.160 or Alpha variants. Del, nucleotide deletion. Nucleotide positions are in reference to the genome of the Wuhan-Hu-1 isolate GenBank accession no. NC_045512.2. (b) Nucleotide diversity is the proportion of sequence reads that do not harbor the consensus (majority) nucleotide. (c) Read depth is the number of reads covering a given nucleotide position.

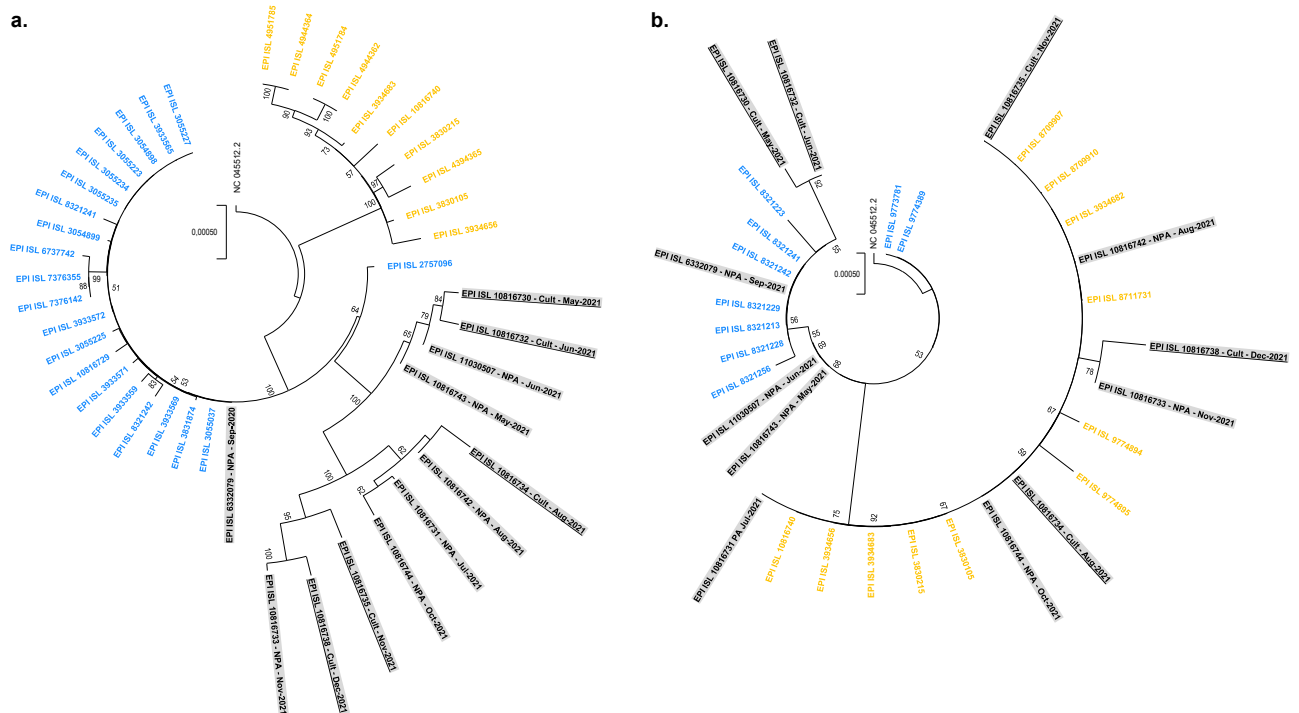


Figure 3. Phylogenetic analyses based on SARS-CoV-2 genomes (a) and spike gene sequences (b). Sequences obtained from the case-patient are indicated by a grey background, and those obtained

from cultures are underlined. Other sequences from our SARS-CoV-2 sequence database are indicated by a blue font when classified as of the B.1.160 variant, and by a yellow font when classified as of the Alpha variant. Sequences are labeled with their GISAID (<https://www.gisaid.org/>; accessed on 18 May 2022) [34] identifiers. Trees are rooted with the genome of the Wuhan-Hu-1 isolate GenBank accession no. NC_045512.2.2.3. Genome of the initial virus.

2.3. Steps in Generation of the Recombinant

We used three procedures to characterize the different recombination steps by analyzing seven sequential respiratory samples collected from the patient (Tables 1 and 2). First, through sequencing from the respiratory samples of the viral genomes; second, sequencing from the respiratory samples of PCR products overlapping the putative recombination sites; third, a viral culture with sequencing of the genomes of the isolates. These approaches allowed us to evidence that several viruses and recombinant forms had coexisted in the sequential samples, as signature mutations of the two variants were co-detected at multiple positions, with a nucleotide diversity that reached high levels and that evolved over time (Figure 2; Supplementary Material: Supplementary Results and Figure S1). We observed an evolution towards the genome sequence of the recombinant virus that predominated at the end of the patient's follow-up, following recombination events at three sites between parental genomes of B.1.160 and Alpha variants, with a low level of nucleotide diversity observed at that time at the positions harboring signature mutations of these variants.

Table 1. Genome sequences obtained from the sequential nasopharyngeal samples of the case-patient.

GISAID Identifier	Sampling Date	Time from Diagnosis (Days)	Next-Generation Sequencing Technology, Instrument
EPI_ISL_6332079	18 September 2020	0	Illumina, NovaSeq
EPI_ISL_10816743	5 May 2021	229	Illumina, NovaSeq
EPI_ISL_11030507	21 June 2021	276	Illumina, NovaSeq
EPI_ISL_10816731	5 July 2021	290	Illumina, NovaSeq
EPI_ISL_10816742	12 August 2021	328	Nanopore, GridION
EPI_ISL_10816744	1 October 2021	378	Illumina, NovaSeq
EPI_ISL_10816733	24 November 2021	432	Illumina, NovaSeq

See also Supplementary Table S3a.

Table 2. Genome sequences obtained from the culture supernatants.

GISAID Identifier	Sampling Date of the Nasopharyngeal Sample	Time to Cytopathic Effect (Days)	Next-Generation Sequencing Technology, Instrument
EPI_ISL_10816730	5 May 2021	8	Illumina, NovaSeq
EPI_ISL_10816732	14 June 2021	4	Illumina, NovaSeq
EPI_ISL_10816734	12 August 2021	4	Illumina, NovaSeq
EPI_ISL_10816735	24 November 2021	5	Illumina, NovaSeq
EPI_ISL_10816738	2 December 2021	7	Illumina, NovaSeq

See also Supplementary Table S3b.

To further support the breakpoints identified between the parental genomes of the Alpha and Marseille-4 variants, we generated Marseille-4 variant/Alpha variant chimeric sequences of the regions overlapping the three putative recombination sites by PCR amplification (Supplementary Material: Figures S3–S5), followed by next-generation sequencing with Nanopore Technology on a gridION instrument, as previously described [27]. For the amplicon corresponding to positions 3100–4570 of the genome, 56 and 87% of the reads were chimeras harboring both Alpha (C3267U) and Marseille-4 (C4543U) signature mutations from the respiratory samples collected in 5 May and in 12 August 2021, respectively (Supplementary Material: Figures S3 and S4). For the amplicon corresponding to positions 24,880–29,010, 70% of the reads were chimeras harboring the Alpha mutation G24914C and the Marseille-4 mutations G25563U, C25710U, C26735U, U26876C and G28975C, and 24% were chimeras harboring the Alpha mutation G24914C and the Marseille-4 mutation

G28975C (Supplementary Material: Figure S5). No PCR amplification was obtained for the region between positions 21,417–23,901. Next-generation sequencing was also carried out using a metagenomic approach with the Nanopore technology to obtain large reads and detect additional Marseille-4 variant/Alpha variant chimeras. For the first previously identified recombination region, four reads with a length ranging between 1855 and 11,979 nucleotides were obtained that harbored signature mutations of the Alpha (C3267U) and Marseille-4 (C4543U) variants. For the third recombination region, four reads with a length between 1486–8143 nucleotides were obtained that harbored signature mutations of the Alpha (G24914C) and Marseille-4 (G25563U) variants (available from URL: <https://www.mediterranee-infection.com/sars-cov-2-recombinant/>; accessed on 18 May 2022). No reads were obtained that covered the Marseille-4 mutation C18877U and the Alpha deletion UACAUG21765. Therefore, several breakpoints between the parental genomes of Alpha and Marseille-4 variants were supported by the presence of chimeric reads.

3. Discussion

We highlight here, in an immunocompromised lymphoma patient chronically infected with SARS-CoV-2 and who received several treatments, the presence of a virus hybrid of two known variants, B.1.160 and Alpha, which successively predominated in our region during the follow-up period of this patient [27,35]. The absence of available samples covering the period between the diagnosis of infection by the B.1.160 variant and first evidence of a hybrid genome did not allow us to date the superinfection by the Alpha variant. The signature mutations of the Alpha variant observed in the hybrid genomes between 8 and 14 months cannot have occurred randomly considering their number, distribution along the genome, and their majority presence, and their location indicates recombinations in three regions. In addition, genomic analyses carried out for sequential respiratory samples and viral cultures demonstrate the successive presence of several viruses with hybrid genomes, one of them having established itself in this patient and the one that continued circulating until his death.

We believe that this observation, which sheds light on the recombination mechanism of RNA viruses, is significant, and to our knowledge, this is the first study describing, through the analysis of sequential samples over more than a year, the generation of recombinant SARS-CoV-2 and its isolation in culture. Sixteen interlineage recombinants between the Alpha variant and non-Alpha viruses were reported in 2021 in the UK, of 279,000 genomes analyzed [8]. In addition, 1175 (0.2%) putative recombinant genomes were identified among 537,360 genomes, and it was reported that up to 5% of SARS-CoV-2 that circulated in the USA and UK might be recombinants [18]. Moreover, the number of cases that capture detection of recombinant genomes is growing [10,13–25], including with recombinant events involving or between Omicron variants [36–39], which highlights the importance of recombination in the evolution of SARS-CoV-2. Besides recombination between SARS-CoV-2 infecting the same human cells, other evolutionary pathways may exist [39]. For instance, different evolutionary trajectories in distinct cell types of the same infected host have been reported [40], and coronaviruses have been reported to harbor a sequence shared with four different families of positive-sense single-stranded RNA viruses and that is putatively shared with insects [41].

Such natural mosaicisms in these viruses make it possible to understand the emergence of RNA viruses and should lead to a strengthening of genomic surveillance in patients, especially in immunocompromised long-term viral carriers, presenting with coinfections by several RNA viruses, as observed in patients infected with several respiratory viruses including SARS-CoV-2, endemic human coronaviruses, influenza viruses, or rhinoviruses [42]. Such infectious episodes could perhaps lead to the emergence of new emerging viruses, as has been, for instance, reported for enteroviruses of humans and great apes [43].

4. Materials and Methods

4.1. SARS-CoV-2 Genome Sequencing

SARS-CoV-2 genome sequencing was performed as previously described. Briefly, viral RNA was extracted from 200 µL of nasopharyngeal swab fluid using the EZ1 Virus Mini kit v2.0 on an EZ1 Advanced XL instrument (Qiagen, Courtaboeuf, France) or using the MagMax Viral/Pathogen Nucleic Acid Isolation kit on the KingFisher Flex system (Thermo Fisher Scientific, Waltham, MA, USA), following the manufacturer's instructions. SARS-CoV-2 genome sequences were obtained by next-generation sequencing with various procedures with the Illumina COVIDSeq protocol on a NovaSeq 6000 instrument (Illumina Inc., San Diego, CA, USA), or by multiplex PCR with ARTIC nCoV-2019 V3 Panel primers (IDT, Coralville, IA, USA) were combined with the Oxford Nanopore technology (ONT) on a GridION instrument (Oxford Nanopore Technologies Ltd., Oxford, UK), as previously described [14,27]. After its extraction, viral RNA was reverse-transcribed according to the COVIDSeq protocol (Illumina Inc., San Diego, CA, USA) or by using the LunaScript RT SuperMix kit (New England Biolabs, Ipswich, MA, USA) when performing next-generation sequencing with the Nanopore technology, following the manufacturer's recommendations.

4.2. Genome Analysis

After using the Nanopore technology combined with the ARTIC protocol, fastq files were processed using the ARTIC field bioinformatics pipeline (ARTIC-nCoV-bioinformatics-SOP-v1.1.0, Nick Loman, Will Rowe, Andrew Rambaut, the ZiBRA Project and the ARTIC project, University of Birmingham, UK, <https://artic.network/ncov-2019/ncov2019-bioinformatics-sop.html>; <https://github.com/artic-network/fieldbioinformatics>; accessed on 18 May 2022), as previously described [14,27]. Next-generation sequencing reads were base-called using Guppy (4.0.14) and were aligned to the genome of the Wuhan-Hu-1 isolate, GenBank accession No. MN908947.3, using minimap2 (v2.17-r941) (<https://github.com/lh3/minimap2>; accessed on 18 May 2022, Dana-Farber Cancer Institute of Boston, USA) [44]. The ARTIC tool align_trim was used to softmask primers from read alignment and cap sequencing depth at a maximum of 400-fold coverage. Consensus-level variant candidates were identified using a threshold of 70% and the Medaka (v.0.11.5) workflow, developed by ARTIC (Nick Loman, Will Rowe, Andrew Rambaut, the ZiBRA Project and the ARTIC project, University of Birmingham, UK, <https://github.com/artic-network/artic-ncov2019>; accessed on 18 May 2022). From the unique sequence obtained with the ARTIC-Nanopore technology, a sorted bam file was loaded on the CLC Genomics workbench v7 software and a tsv file was then exported. NovaSeq reads were basecalled using the Dragen Bcl Convert pipeline (v3.9.3; https://emea.support.illumina.com/sequencing/sequencing_software/bcl-convert.html; accessed on 18 May 2022 (Illumina Inc., San Diego, CA, USA). Mapping was carried out on the Wuhan-Hu-1 isolate genome with the bwa-mem2 tool (v2.2.1; <https://github.com/bwa-mem2/bwa-mem2>; accessed on 18 May 2022, Heng Li, Harvard, USA) and was cleaned with Samtools (v1.13; <https://www.htslib.org/>; accessed on 18 May 2022) [45]. Variant calling was performed with freebayes (v1.3.5; <https://github.com/freebayes/freebayes>; accessed on 18 May 2022, Erik Garrison, Gabor Marth, University of Tennessee and Utah) [46] and consensus genomes were built with Bcftools (v1.13; <https://samtools.github.io/bcftools/bcftools.html>; accessed on 18 May 2022, 2012–2021 Genome Research Ltd.). Freebayes results were filtered with a threshold of 70% for the majority nucleotide. A tsv file was generated using an in-house Python script. The clade was designated at the consensus level with the Nextclade online tool (<https://clades.nextstrain.org/>; accessed on 18 May 2022, 2020 Nextstrain developers, Swiss Institute of Bioinformatics) [32,47] and an in-house Python script allowed for the detection of variants and the hybrids of variants. At the sub-consensus level, variant frequencies that were compared to the Wuhan-Hu-1 isolate genome were calculated from tsv files. Nucleotide diversity at genomic positions was calculated using the Microsoft Excel software (<https://www.microsoft.com/en-us/microsoft-365/excel>; accessed on 18 May 2022, Microsoft Corporation, Redmond, WA, USA) with an in-house built

file. It corresponded to the proportion of sequence reads that do not harbor the consensus (majority) nucleotide. Genome sequences obtained in the present study were submitted to the GISAID sequence database (<https://www.gisaid.org/>; accessed on 18 May 2022, 2008–2022, Freunde von GISAID e.V. Munich, Germany) [34] (see Supplementary Material: Supplementary Table S1).

4.3. Generation of Additional Sequence Reads

Sequencing of reverse-transcription-PCR-targeted regions: extraction of the RNA samples was carried out using the EZ1 Virus kit with the EZ1 Advanced XL instrument (Qiagen) following the manufacturer's recommendations. PCR amplification of the 3 regions was amplified in a 25 µL total volume using the SuperScript III One-Step RT-PCR Kit (Invitrogen, Carlsbad, CA, USA), using primer concentrations of 200 nM per reaction. PCR were performed with following conditions: 50 °C for 25 min, 95 °C for 2 min, then 40 cycles including 15 s at 95 °C, 45 s at 60 °C, and 2 min at 68 °C. Sequences of PCR primers are provided in the Supplementary Material. Amplicons were sequenced with Nanopore technology on a GridION instrument (Oxford Nanopore Technologies Ltd., Oxford, UK), following the manufacturer's instructions. Fastq files were processed as described above. Continuous reads overlapping signature mutations of distinct variants were filtered using SAMtools (v1.13; <https://github.com/samtools/2008-2022> Genome Research Ltd., accessed on 18 May 2022) [45] combined with an in-house awk script. Reads were then filtered according to variant-specific nucleotide patterns using SAMtools combined with an in-house awk script. Groups of reads with same patterns of mutations were then visualized using the IGV software (<https://software.broadinstitute.org/software/igv/>; accessed on 18 May 2022, Broad Institute and the Regents of the University of California, USA) [48].

Metagenomic sequencing: nucleic acid extraction was performed with the EZ1 Virus kit with the EZ1 Advanced XL instrument (Qiagen) following the manufacturer's recommendations, using 200 µL of sample and eluting in 60 µL of elution buffer. Reverse transcription was performed with all 60 µL of this solution using the TaqMan Reverse Transcription Reagent kit (Applied-Biosystems, Foster City, CA, USA), according to the manufacturer's protocol under the following conditions: 10 min at 25 °C, 30 min at 48 °C, and 5 min at 95 °C. Then, 300 µL of obtained cDNA was transferred to a 1.5 mL Eppendorf LoBind tube (Eppendorf, Le Pecq, France). Second DNA strand was synthesized by adding a mix of 24 µL of Klenow Fragment DNA polymerase (New England Biolabs, Beverly, MA, USA), 66 µL of nuclease-free water, 45 µL of NEB Buffer 2 (New England Biolabs, Ipswich, MA, USA), and 15 µL of dNTPs working solution produced with 10 µL of each dNTP at a 100 mM concentration, and 60 µL of nuclease-free water (New England Biolabs, Ipswich, MA, USA). This mix was kept at 37 °C for one hour. A purification step consisted of adding 450 µL of magnetic CleanNGS beads for a 1:1 volume ratio (CleanNA, Waddinxveen, the Netherlands) then incubating them for 5 min in a magnetic support, and washing with 1000 µL of ethanol at 70%, before elution of the beads was performed in 50 µL of Tris EDTA 1X with centrifugation for 10 min at 300 rpm at room temperature. Subsequently, a DNA library was prepared with the DNA ligation sequencing kit SQK-LSK109 (Oxford Nanopore Technologies Ltd., Oxford, UK), and next-generation sequencing was performed with the Nanopore technology on a PromethION instrument (Oxford Nanopore Technologies Ltd., Oxford, UK). Each sample was sequenced on a different PromethION Flow cell R10.4 (Oxford Nanopore Technologies Ltd., Oxford, UK).

4.4. Phylogenetic Analysis Based on Whole and Partial Genome Sequences

Phylogenetic analyses were performed separately for the twelve genome sequences and the twelve spike gene sequences obtained from the nasopharyngeal samples or the culture supernatants. Sequences were aligned using MAFFT v.7 (Kazutaka Katoh and Daron M Standley, Osaka University, Japan) [49] with their 20 most similar hits identified with the BLAST tool (National Library of Medicine, Rockville Pike, MD, USA) [50] among SARS-CoV-2 genomes from our database, which contains sequences obtained

from clinical samples collected between February 2020 and February 2022 [14,27]. Phylogeny reconstruction was performed using the IQ-TREE software with the GTR Model and 1000 ultrafast bootstrap repetitions (<http://www.iqtree.org>, Free Software Foundation, Boston, MA, USA) [51], and trees were visualized with iTOL (Interactive Tree of Life) (<https://itol.embl.de/>; accessed on 18 May 2022, EMBL 2022) [52] and MEGA X (v10.2.6; <https://www.megasoftware.net/>; accessed on 18 May 2022, 2007 Free Software Foundation) [53] softwares.

4.5. Virus Culture Isolation

Culture isolation was performed on Vero E6 cells, as previously described [33]. Briefly, 500 µL of nasopharyngeal swab fluid was passed through a centrifugal filter with a pore size of 0.22-µm (Merck Millipore, Darmstadt, Germany) before the inoculation of 100 µL of filtrate was performed in 4 wells of culture microplates with 96 wells that contained Vero E6 cells (ATCC CRL-1586) in Minimum Essential Medium culture medium, comprising 4% fetal calf serum and 1% glutamine. After a centrifugation step at 4000× *g*, culture microplates were incubated at 37 °C and were observed daily with an inverted microscope for evidence of cytopathogenic effect. We attempted, without success, to isolate the parental Alpha variant from respiratory samples collected in 2021 from the case-patient by selecting this virus through inoculating the respiratory samples with neutralizing serum from a convalescent individual previously infected by the B.1.160 variant, as previously reported [54], at equal volumes (50 µL of filtered respiratory sample and 50 µL of serum).

Supplementary Materials: The following supporting information can be downloaded at: <https://www.mdpi.com/article/10.3390/v14061266/s1>. Additional Methods, Results, Figure S1: Virological follow-up by real-time reverse transcription PCR (qPCR) targeting SARS-CoV-2 RNA for the patient, Figure S2: Majority nucleotides and nucleotide diversity for sequences obtained from the respiratory samples and the culture supernatant at nucleotide positions of the SARS-CoV-2 genome that harbor signature mutations of the B.1.160 or Alpha variants and at any other positions that harbor mutations (a), and sequencing depth at nucleotide positions (b), Figure S3: Detailed content of amplicons corresponding to positions 3100–4570 of the SARS-CoV-2 genome and retrieved from respiratory samples collected on 5 May 2021, Figure S4: Detailed content of amplicons corresponding to positions 3100–4570 of the SARS-CoV-2 genome and retrieved from respiratory samples collected on 12 August 2021, Figure S5: Detailed content of amplicons corresponding to positions 24,880–29,010 of the SARS-CoV-2 genome and retrieved from respiratory samples collected on 12 August 2021, Table S1: List of GISAID identifiers for sequences used in the present study, and Table S2: Sampling time and location for sequences used in the present study, Table S3: Identifiers of raw data deposited in the European Bioinformatics Institute (EMBL-EBI) sequence database (<https://www.ebi.ac.uk/>; accessed on 18 May 2022), and References, are provided in the Supplementary Material.

Author Contributions: P.C., B.L.S. and D.R. conceived the project. E.B., P.C., J.-C.L., A.L., M.B. and P.L.-M. provided materials or performed analyses. E.B., P.C., J.-C.L., A.L., M.B., P.-E.F., B.L.S. and D.R. analyzed the data. E.B., P.C., P.-E.F., B.L.S. and D.R. drafted the paper. All authors have read and agreed to the published version of the manuscript.

Funding: This work was supported by the French Government under the “Investments for the Future” program managed by the National Agency for Research (ANR) (Méditerranée-Infection 10-IAHU-03), by the Région Provence Alpes Côte d’Azur and European funding FEDER PRIMMI (Fonds Européen de Développement Régional-Plateformes de Recherche et d’Innovation Mutualisées Méditerranée Infection) (FEDER PA 0000320 PRIMMI), and by the French Ministry of Higher Education, Research and Innovation (ministère de l’Enseignement supérieur, de la Recherche et de l’Innovation) and the French Ministry of Solidarity and Health (Ministère des Solidarités et de la Santé).

Institutional Review Board Statement: This study has been approved by the ethics committee of University Hospital Institute (IHU) Méditerranée Infection (No. 2022-008). Access to the patients’ biological and registry data issued from the hospital information system was approved by the data protection committee of Assistance Publique-Hôpitaux de Marseille (APHM) and was recorded in the European General Data Protection Regulation registry under number RGPD/APHM 2019-73.

Informed Consent Statement: This study has been approved by the ethics committee of University Hospital Institute (IHU) Méditerranée Infection (No. 2022-008). Access to the patients' biological and registry data issued from the hospital information system was approved by the data protection committee of Assistance Publique-Hôpitaux de Marseille (APHM) and was recorded in the European General Data Protection Regulation registry under number RGPD/APHM 2019-73.

Data Availability Statement: The dataset generated and analyzed during the current study is available in the GISAID sequence database (<https://www.gisaid.org/>; accessed on 18 May 2022, 2008–2022, Freunde von GISAID e.V. Munich, Germany) [34].

Acknowledgments: We are thankful to Ludivine Brechard, Claudia Andrieu, Raphael Tola, Jeremy Delerce for their technical help; to Sophie Amrane and Justine Raclot for their help with the clinical management; and to the medical biology laboratory Alphabio, hôpital Européen, Marseille, France, for providing some results of SARS-CoV-2 qPCR testing.

Conflicts of Interest: The authors have no conflict of interest to declare relative to the present study. Didier Raoult was a consultant for the Hitachi High-Technologies Corporation, Tokyo, Japan from 2018 to 2020. He is a scientific board member of the Eurofins company and a founder of a microbial culture company (Culture Top). Funding sources had no role in the design and conduct of the study, the collection, management, analysis, and interpretation of the data, and the preparation, review, or approval of the manuscript.

References

1. Xiao, Y.; Rouzine, I.M.; Bianco, S.; Acevedo, A.; Goldstein, E.F.; Farkov, M.; Andino, R. RNA Recombination Enhances Adaptability and Is Required for Virus Spread and Virulence. *Cell Host Microbe* **2017**, *22*, 420. [CrossRef] [PubMed]
2. Bentley, K.; Evans, D.J. Mechanisms and consequences of positive-strand RNA virus recombination. *J. Gen. Virol.* **2018**, *99*, 1345–1356. [CrossRef] [PubMed]
3. Lai, M.M.C. Recombination in large RNA viruses: Coronaviruses. *Semin. Virol.* **1996**, *7*, 381–388. [CrossRef]
4. Zhang, Y.; Li, J.; Xiao, Y.; Zhang, J.; Wang, Y.; Chen, L.; Paranhos-Baccalà, G.; Ren, L.; Wang, J. Genotype shift in human coronavirus OC43 and emergence of a novel genotype by natural recombination. *J. Infect.* **2015**, *70*, 641–650. [CrossRef] [PubMed]
5. So, R.T.; Chu, D.K.; Miguel, E.; Perera, R.A.; Oladipo, J.O.; Fassi-Fihri, O.; Peiris, M. Diversity of Dromedary Camel Coronavirus HKU23 in African Camels Revealed Multiple Recombination Events among Closely Related Betacoronaviruses of the Subgenus Embecovirus. *J. Virol.* **2019**, *93*, e01236-19. [CrossRef] [PubMed]
6. Gribble, J.; Stevens, L.J.; Agostini, M.L.; Anderson-Daniels, J.; Chappell, J.D.; Lu, X.; Pruijssers, A.J.; Routh, A.L.; Denison, M.R. The coronavirus proofreading exoribonuclease mediates extensive viral recombination. *PLoS Pathog.* **2021**, *17*, e1009226. [CrossRef] [PubMed]
7. Zhu, Z.; Meng, K.; Meng, G. Genomic recombination events may reveal the evolution of coronavirus and the origin of SARS-CoV-2. *Sci. Rep.* **2020**, *10*, 21617. [CrossRef]
8. Jackson, B.; Boni, M.F.; Bull, M.J.; Colleran, A.; Colquhoun, R.M.; Darby, A.C.; Rambaut, A. Generation and transmission of interlineage recombinants in the SARS-CoV-2 pandemic. *Cell* **2021**, *184*, 5179–5188.e8. [CrossRef]
9. Francisco, R.D.S., Jr.; Benites, L.F.; Lamarca, A.P.; de Almeida, L.G.; Hansen, A.W.; Gularte, J.S.; Demoliner, M.; Gerber, A.L.; Guimarães, A.P.D.C.; Antunes, A.K.E.; et al. Pervasive transmission of E484K and emergence of VUI-NP13L with evidence of SARS-CoV-2 co-infection events by two different lineages in Rio Grande do Sul, Brazil. *Virus Res.* **2021**, *296*, 198345. [CrossRef]
10. Taghizadeh, P.; Salehi, S.; Heshmati, A.; Houshmand, S.M.; InanlooRahatloo, K.; Mahjoubi, F.; Sanati, M.H.; Yari, H.; Alavi, A.; Jamehdar, S.A.; et al. Study on SARS-CoV-2 strains in Iran reveals potential contribution of co-infection with and recombination between different strains to the emergence of new strains. *Virology* **2021**, *562*, 63–73. [CrossRef]
11. Rockett, R.J.; Draper, J.; Gall, M.; Sim, E.M.; Arnott, A.; Agius, J.E.; Sintchenko, V. Co-infection with SARS-CoV-2 Omicron and Delta Variants revealed by genomic surveillance. *Nat. Commun.* **2022**, *13*, 2745. [CrossRef] [PubMed]
12. Musso, N.; Maugeri, J.G.; Bongiorno, D.; Stracquadanio, S.; Bartoloni, G.; Stefani, S.; Di Stefano, E.D. SARS-CoV-2's high rate of genetic mutation under immune selective pressure: From oropharyngeal B.1.1.7 to intrapulmonary B.1.533 in a post-vaccine patient. *Int. J. Infect. Dis.* **2022**, *118*, 169–172. [CrossRef] [PubMed]
13. He, Y.; Ma, W.; Dang, S.; Chen, L.; Zhang, R.; Mei, S.; Wei, X.; Lv, Q.; Peng, B.; Chen, J.; et al. Possible recombination between two variants of concern in a COVID-19 patient. *Emerg. Microbes Infect.* **2022**, *11*, 552–555. [CrossRef] [PubMed]
14. Colson, P.; Fournier, P.E.; Delerce, J.; Million, M.; Bedotto, M.; Houhamdi, L.; La Scola, B. Culture and identification of a "Deltamicron" SARS-CoV-2 in a three cases cluster in southern France. *J. Med. Virol.* **2022**; Online ahead of print. [CrossRef]
15. Yi, H. 2019 Novel Coronavirus Is Undergoing Active Recombination. *Clin. Infect. Dis.* **2020**, *71*, 884–887. [CrossRef]
16. Yeh, T.Y.; Contreras, G.P. Emerging viral mutants in Australia suggest RNA recombination event in the SARS-CoV-2 genome. *Med. J. Aust.* **2020**, *213*, 44. [CrossRef]
17. Gallaher, W.R. A palindromic RNA sequence as a common breakpoint contributor to copy-choice recombination in SARS-COV-2. *Arch. Virol.* **2020**, *165*, 2341–2348. [CrossRef]

18. VanInsberghe, D.; Neish, A.S.; Lowen, A.C.; Koelle, K. Recombinant SARS-CoV-2 genomes are currently circulating at low levels. *bioRxiv* **2021**. [[CrossRef](#)]
19. Haddad, D.; John, S.E.; Mohammad, A.; Hammad, M.M.; Hebbbar, P.; Channanath, A.; Al-Mulla, F. SARS-CoV-2: Possible recombination and emergence of potentially more virulent strains. *PLoS ONE* **2021**, *16*, e0251368. [[CrossRef](#)]
20. Varabyou, A.; Pockrandt, C.; Salzberg, S.L.; Pertea, M. Rapid detection of inter-clade recombination in SARS-CoV-2 with Bolotie. *Genetics* **2021**, *218*, iyab074. [[CrossRef](#)]
21. Leary, S.; Gaudieri, S.; Parker, M.D.; Chopra, A.; James, I.; Pakala, S.; Sette, A. Generation of a novel SARS-CoV-2 sub-genomic RNA due to the R203K/G204R variant in nucleocapsid: Homologous recombination has potential to change SARS-CoV-2 at both protein and RNA level. *bioRxiv* **2021**. [[CrossRef](#)]
22. Lohrasbi-Nejad, A. Detection of homologous recombination events in SARS-CoV-2. *Biotechnol. Lett.* **2022**, *17*, 399–414. [[CrossRef](#)] [[PubMed](#)]
23. Kreier, F. Deltacron: The story of the variant that wasn't. *Nature* **2022**, *602*, 19. [[CrossRef](#)] [[PubMed](#)]
24. Ignatieva, A.; Hein, J.; Jenkins, P.A. Ongoing Recombination in SARS-CoV-2 Revealed through Genealogical Reconstruction. *Mol. Biol. Evol.* **2022**, *39*, msac028. [[CrossRef](#)] [[PubMed](#)]
25. Sekizuka, T.; Itokawa, K.; Saito, M.; Shimatani, M.; Matsuyama, S.; Hasegawa, H.; Saito, T.; Kuroda, M. Genome Recombination between Delta and Alpha Variants of Severe Acute Respiratory Syndrome Coronavirus 2 (SARS-CoV-2). *Jpn. J. Infect. Dis.* **2022**; Online ahead of print. [[CrossRef](#)] [[PubMed](#)]
26. Million, M.; Lagier, J.-C.; Tissot-Dupont, H.; Ravaux, I.; Dhiver, C.; Tomei, C.; Cassir, N.; Delorme, L.; Cortaredona, S.; Amrane, S.; et al. Early combination therapy with hydroxychloroquine and azithromycin reduces mortality in 10,429 COVID-19 outpatients. *Rev. Cardiovasc. Med.* **2021**, *22*, 1063–1072. [[CrossRef](#)] [[PubMed](#)]
27. Colson, P.; Fournier, P.-E.; Chaudet, H.; Delerce, J.; Giraud-Gatineau, A.; Houhamdi, L.; Andrieu, C.; Brechard, L.; Bedotto, M.; Prudent, E.; et al. Analysis of SARS-CoV-2 Variants From 24,181 Patients Exemplifies the Role of Globalization and Zoonosis in Pandemics. *Front. Microbiol.* **2022**, *12*, 786233. [[CrossRef](#)]
28. Brouqui, P.; Colson, P.; Melenotte, C.; Houhamdi, L.; Bedotto, M.; Devaux, C.; Gautret, P.; Million, M.; Parola, P.; Stoupan, D.; et al. COVID-19 re-infection. *Eur. J. Clin. Investig.* **2021**, *51*, e13537. [[CrossRef](#)]
29. Drancourt, M.; Cortaredona, S.; Melenotte, C.; Amrane, S.; Eldin, C.; La Scola, B.; Parola, P.; Million, M.; Lagier, J.-C.; Raoult, D.; et al. SARS-CoV-2 Persistent Viral Shedding in the Context of Hydroxychloroquine-Azithromycin Treatment. *Viruses* **2021**, *13*, 890. [[CrossRef](#)]
30. Colson, P.; Devaux, C.A.; Lagier, J.C.; Gautret, P.; Raoult, D. A Possible Role of Remdesivir and Plasma Therapy in the Selective Sweep and Emergence of New SARS-CoV-2 Variants. *J. Clin. Med.* **2021**, *10*, 3276. [[CrossRef](#)]
31. Rambaut, A.; Holmes, E.C.; O'Toole, Á.; Hill, V.; McCrone, J.T.; Ruis, C.; du Plessis, L.; Pybus, O.G. A dynamic nomenclature proposal for SARS-CoV-2 lineages to assist genomic epidemiology. *Nat. Microbiol.* **2020**, *5*, 1403–1407. [[CrossRef](#)]
32. Aksamentov, I.; Roemer, C.; Hodcroft, E.B.; Neher, R.A. Nextclade: Clade assignment, mutation calling and quality control for viral genomes. *J. Open Source Softw.* **2021**, *6*, 3773. [[CrossRef](#)]
33. La Scola, B.; Le Bideau, M.; Andreani, J.; Hoang, V.T.; Grimaldier, C.; Colson, P.; Raoult, D. Viral RNA load as determined by cell culture as a management tool for discharge of SARS-CoV-2 patients from infectious disease wards. *Eur. J. Clin. Microbiol. Infect. Dis.* **2020**, *39*, 1059–1061. [[CrossRef](#)] [[PubMed](#)]
34. Alm, E.; Broberg, E.K.; Connor, T.; Hodcroft, E.B.; Komissarov, A.B.; Maurer-Stroh, S.; Pereyaslov, D. Geographical and temporal distribution of SARS-CoV-2 clades in the WHO European Region, January to June 2020. *Euro. Surveill.* **2020**, *25*, 2001410. [[CrossRef](#)]
35. Fournier, P.E.; Colson, P.; Levasseur, A.; Devaux, C.A.; Gautret, P.; Bedotto, M.; Raoult, D. Emergence and outcomes of the SARS-CoV-2 'Marseille-4' variant. *Int. J. Infect. Dis.* **2021**, *106*, 228–236. [[CrossRef](#)] [[PubMed](#)]
36. Ou, J.; Lan, W.; Wu, X.; Zhao, T.; Duan, B.; Yang, P.; Ren, Y.; Quan, L.; Zhao, W.; Seto, D.; et al. Tracking SARS-CoV-2 Omicron diverse spike gene mutations identifies multiple inter-variant recombination events. *Signal Transduct. Target. Ther.* **2022**, *7*, 138. [[CrossRef](#)] [[PubMed](#)]
37. Gu, H.; Ng, D.Y.; Liu, G.Y.; Cheng, S.S.; Krishnan, P.; Chang, L.D.; Poon, L. Samuel SM Cheng, Pavithra Krishnan, Lydia DJ Chang, Sammi SY Cheuk, Mani MY Hui, Tommy TY Lam, Malik Peiris, Leo Poon. Detection of a BA.1/BA.2 recombinant in travelers arriving in Hong Kong, February 2022. *medRxiv* **2022**. [[CrossRef](#)]
38. Colson, P.; Delerce, J.; Marion-Paris, E.; Lagier, J.C.; Levasseur, A.; Fournier, P.E.; Raoult, D. A 21L/BA.2-21K/BA.1 "MixOmicron" SARS-CoV-2 hybrid undetected by qPCR that screen for variant in routine diagnosis. *medRxiv* **2022**. [[CrossRef](#)]
39. Perez, J.C.; Lounnas, V.; Montagnier, L. The Omicron variant breaks the evolutionary lineage of SARS-CoV-2 variants. *Int. J. Res. Granthaalayah* **2021**, *9*, 108–132. [[CrossRef](#)]
40. Gupta, K.; Toelzer, C.; Williamson, M.K.; Shoemark, D.K.; Oliveira, A.S.F.; Matthews, D.A.; Berger, I. Structural insights in cell-type specific evolution of intra-host diversity by SARS-CoV-2. *Nat. Commun.* **2022**, *13*, 222. [[CrossRef](#)]
41. Tengs, T.; Delwiche, C.F.; Monceyron Jonassen, C. A genetic element in the SARS-CoV-2 genome is shared with multiple insect species. *J. Gen. Virol.* **2021**, *102*, 001551. [[CrossRef](#)]
42. Le Glass, E.; Hoang, V.T.; Boschi, C.; Ninove, L.; Zandotti, C.; Boutin, A.; Colson, P. Incidence and Outcome of Coinfections with SARS-CoV-2 and Rhinovirus. *Viruses* **2021**, *13*, 2528. [[CrossRef](#)] [[PubMed](#)]

43. Amona, I.; Medkour, H.; Akiana, J.; Davoust, B.; Tall, M.L.; Grimaldier, C.; Mediannikov, O. Enteroviruses from Humans and Great Apes in the Republic of Congo: Recombination within Enterovirus C Serotypes. *Microorganisms* **2020**, *8*, 1779. [[CrossRef](#)] [[PubMed](#)]
44. Li, H. Minimap2: Pairwise alignment for nucleotide sequences. *Bioinformatics* **2018**, *34*, 3094–3100. [[CrossRef](#)] [[PubMed](#)]
45. Danecek, P.; Bonfield, J.K.; Liddle, J.; Marshall, J.; Ohan, V.; Pollard, M.O.; Whitwham, A.; Keane, T.; A. McCarthy, S.; Davies, R.M.; et al. Twelve years of SAMtools and BCFtools. *GigaScience* **2021**, *10*, giab008. [[CrossRef](#)]
46. Garrison, E.; Marth, G. Haplotype-Based variant detection from short-read sequencing. *arXiv* **2012**, arXiv:1207.3907.
47. Hadfield, J.; Megill, C.; Bell, S.M.; Huddleston, J.; Potter, B.; Callender, C. Nextstrain: Real-time tracking of pathogen evolution. *Bioinformatics* **2018**, *34*, 4121–4123. [[CrossRef](#)]
48. Robinson, J.T.; Thorvaldsdottir, H.; Wenger, A.M.; Zehir, A.; Mesirov, J.P. Variant Review with the Integrative Genomics Viewer (IGV). *Cancer Res.* **2017**, *77*, 31–34. [[CrossRef](#)]
49. Katoh, K.; Standley, D.M. MAFFT multiple sequence alignment software version 7: Improvements in performance and usability. *Mol. Biol. Evol.* **2013**, *30*, 772–780. [[CrossRef](#)]
50. Altschul, S.F.; Gish, W.; Miller, W.; Myers, E.W.; Lipman, D.J. Basic local alignment search tool. *J. Mol. Biol.* **1990**, *215*, 403–410. [[CrossRef](#)]
51. Minh, B.Q.; Schmidt, H.A.; Chernomor, O.; Schrempf, D.; Woodhams, M.D.; von Haeseler, A.; Lanfear, R. IQ-TREE 2: New Models and Efficient Methods for Phylogenetic Inference in the Genomic Era. *Mol. Biol. Evol.* **2020**, *37*, 1530–1534. [[CrossRef](#)]
52. Letunic, I.; Bork, P. Interactive tree of life (iTOL) v3: An online tool for the display and annotation of phylogenetic and other trees. *Nucleic Acids Res.* **2016**, *44*, W242–W245. [[CrossRef](#)] [[PubMed](#)]
53. Kumar, S.; Stecher, G.; Li, M.; Nnyaz, C.; Tamura, K. MEGA X: Molecular Evolutionary Genetics Analysis across Computing Platforms. *Mol. Biol. Evol.* **2018**, *35*, 1547–1549. [[CrossRef](#)] [[PubMed](#)]
54. Jaafar, R.; Boschi, C.; Aherfi, S.; Bancod, A.; Le Bideau, M.; Edouard, S.; La Scola, B. High individual heterogeneity of neutralizing activities against the original strain and nine different variants of SARS-CoV-2. *Viruses* **2021**, *13*, 2177. [[CrossRef](#)] [[PubMed](#)]